



On the Aerodynamic and Acoustic Behavior of Double Outlet Squirrel Cage Fans

M. Mahmoodi and N. Montazerin[†]

School of Mechanical Engineering, Amirkabir University of Technology, Tehran, Iran

[†]*Corresponding Author Email: mntzrn@aut.ac.ir*

(Received December 13, 2019; accepted May 7, 2020)

ABSTRACT

Investigations and observations on fluid flow and performance characteristics (numerically and experimentally) and sound generation (experimentally) of single and double outlet squirrel cage fans are performed in this study. The main objective is to survey the performance of double outlet fans and the effect of two volute tongues as main sound sources. Fan performance and sound experiments are conducted using an in-duct experimental setup. The efficiency and pressure curves show that each outlet channels of the double outlet fan operates similar to a single outlet one. As a criterion for evaluating the sound generation, total sound pressure level (SPL) and the noise component at blade passing frequency (BPF) in the power spectrum are considered. A comparison between the total sound pressure levels of the fans shows that in both of them the BPF noise increases with flow rate, while higher SPL is found for the double outlet one. An exactly-higher velocity jet/wake flow from the rotor in double outlet fan is responsible for the higher BPF noise.

Keywords: Fan, Forward curved; Double outlet; Efficiency; Sound pressure level; Blade passing frequency; Flow induced noise.

NOMENCLATURE

b	rotor width	Q	flow rate
B	volute width	r	volute radius
BPF	Blade Passing Frequency	$r_{in\ tip}$	inlet tip radius
BPF noise	SPL at Blade Passing Frequency	r_s	radius of start of the cutoff
BEP	Best Efficiency Point	r_v	radius of the volute tongue tip
D_1	rotor inner diameter	u_i, u_j	mean velocity component
D_2	rotor outer diameter	u'_i, u'_j	fluctuating velocity
D_{inlet}	fan inlet diameter	U	upper channel
d_s	impeller-volute tongue clearance	Z	number of blades
h	fan outlet height	α_s	volute spread angle
k_p	compressibility coefficient	β_1	blade inlet angle
L	lower channel	β_2	blade outlet angle
N	rotational speed	η	efficiency
n	rotational speed	θ	volute angle
SPL	Sound Pressure Level	θ_s	volute start angle
SPL_Σ	total SPL, total noise	ρ	density
SPL_{ave}	average sound pressure level	φ	flow coefficient
P	sound pressure	ψ	total pressure coefficient
P_{ref}	reference pressure	δ_{ij}	Kronecker delta
PR	motor power		
P_t	total pressure		

1. INTRODUCTION

Squirrel cage fans are composed of a volute and a forward-curved blade centrifugal rotor (Fig. 1).

Some main practical characteristics of these fans are relatively high volumetric flow rate, simple construction, and low cost of production. In these fans the flow enters the fan axially from the shroud

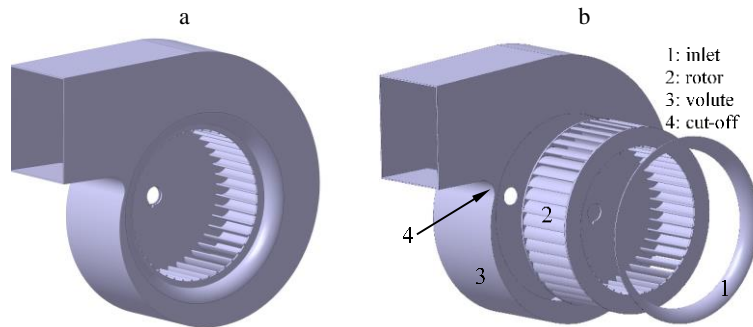


Fig. 1. A view of squirrel cage fan; (a) a complete setup, (b) a detailed view.

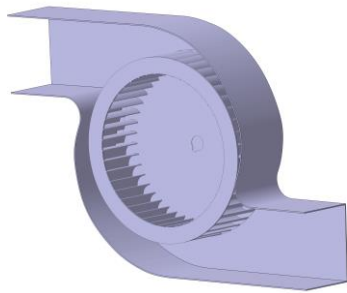


Fig. 2. A schematic view of double outlet squirrel cage fan volute.

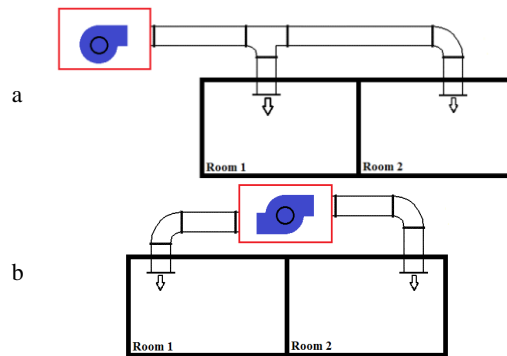


Fig. 3. Applications of (a) double outlet and (b) single outlet squirrel cage fans, in a ventilating system.

side and gradually turns into radial direction (Damangir and Montazerin 1998; Montazerin *et al.* 2001; Montazerin *et al.* 2015; Wang *et al.* 2018; Jiang *et al.* 2018). Even the best available configuration gives poor flow guidance and inefficient energy exchange inside these fans. High angle of incidence, the mismatch between the inlet and the impeller and non-uniform flow at impeller inlet, result in extensive unsteady separation over the blade suction side and inside the volute (Montazerin *et al.* 2015; Wang *et al.* 2018).

These fans are widely employed in ventilating and air conditioning systems such as air handling units and evaporative coolers (Bleier 1998; Cory 2005). The fan of a central unit in heating and ventilating industry usually supplies more than one outlet port. The squirrel cage fan also produces a relatively large volume of air and supplies more than one ventilating space. Automobile ventilation is an example where such fans serve both right and left sides of the cabin.

The volute of squirrel cage fan collects flow from the rotor exit and delivers it to the outlet channel (Montazerin *et al.* 2015; Jiang *et al.* 2018). A double outlet centrifugal fan that can be installed between the delivery ports has a volute with two outlet ports (Fig. 2) and allows less turning in the channels after the fan. It is also provides more flexibility regarding its positioning and the required

space (Fig. 3). When the fan internal fluid path is compared with single outlet fans, the flow only undergoes half the rotation inside the volute.

The idea is not strange to centrifugal turbomachines. Some centrifugal compressors of reciprocating engine turbochargers have many outlets that each outlet supplies air to a different engine cylinder.

The fundamental question about double outlet squirrel cage fan is their performance and acoustic behavior in comparison with single outlet type. The main contributors of sound sources in fans are the forces acting on blades, vanes and casing (Montazerin *et al.* 2015; Hessami Azizi *et al.* 2005; Paramasivam *et al.* 2017; Joonga *et al.* 2019). These forces can be periodic or random, and consequently the power spectrum of the fan sound pressure level (SPL) represents both discrete and broad band components. The flow-induced noise in centrifugal fans originates from three different sources: turbulent stress (quadruple), steady and unsteady forces exerted by solid surfaces on the flow (dipole), and volume displacement effects of the moving surfaces (monopole) (Montazerin *et al.* 2015; Hessami Azizi *et al.* 2005). The discrete noise components that are known as tonal noise, are found at blade passing frequency (BPF) and its harmonics. The tonal noise originates from the interaction between the non-uniform flow leaving

the rotor (the fluid flow with continuous jet and wake profile) and the casing especially around the volute tongue. The broad band components are generated due to the inlet separated flow, reverse flow, separated flow and the vortex shedding at the impeller blade trailing edges. In centrifugal fans, the discrete frequency components (BPF noise) are more significant as compared to broad band noise (Paramasivam *et al.* 2017; Jian *et al.* 2018; Xu and Mao 2016a).

A review of the literature on sound generation and improvement of acoustic behavior of centrifugal fan shows the main effect of volute tongue noise. Neise (1992) stated that increasing the distance between the impeller and volute tongue (impeller – volute tongue clearance) could decrease the tonal noise intensity. Velarde-Suárez *et al.* (1999) conducted an experimental study to investigate the aero-acoustic behavior of forward-curved blades centrifugal fans. They found that in the noise spectra, the BPF component increases with flow rate. In another experimental work Velarde-Suárez *et al.* (2006) determined sources of tonal noise in a backward-curved centrifugal fan. They found that the interaction between the fluctuating flow leaving the impeller and the volute tongue is a strong source of noise. Influence of geometric features on the acoustic behavior of a squirrel cage fan was investigated experimentally by Velarde-Suárez *et al.* (2008). They found some cut-off configurations that were able to reduce fan noise without reducing operating range. Qi *et al.* (2009) and Qi and Wei (2017) investigate the effects of inclined volute tongue, impeller-volute tongue clearance, and hub-volute clearance on performance and noise of forward-curved centrifugal fan. They observe that an inclined tongue could reduce fan noise while deteriorate total pressure. Finally they state that the effects of volute-tongue geometry and hub – impeller clearance on fan performance and noise could not be simply added. Some experiments on centrifugal fan noise reduction by an absorbing foam on the volute tongue were conducted by Gu *et al.* (2011) and Xu and Mao (2016a,b). It is also confirmed the main effect of BPF noise (volute tongue effects) in centrifugal pumps (Liu *et al.* 2016; Gao *et al.* 2017) and compressors (Zhoua *et al.* 2018; Zhang *et al.* 2018; Liu *et al.* 2019), similar to the centrifugal fans.

The fluid flow, performance and acoustical behavior of double outlet squirrel cage fan in comparison with a single outlet one are missing in literature. As mentioned before, in double outlet fan the volute length from cut-off to outlet channel is less than half of that in case of single outlet fan, and subsequently rotor exit flow only undergoes half the rotation inside the volute and friction loss due to fluid flow along the volute is less than the single outlet one. On the other hand a double outlet fan has two volute tongues and consequently two tonal noise sources. Differences in fluid flow should be investigated when a twin volute is used instead of a common volute in squirrel cage fan.

The purpose of the present work is to survey the influence of volute with two outlets on aerodynamic

noise and performance of a single inlet squirrel cage rotor. For these purposes a double outlet (fan with two volute tongue) and a single outlet fan with similar rotor, volute curve and impeller – volute tongue clearance are considered. Both numerical and experimental tools are employed in this research to clarify unknown aspect of the considered phenomena. At first fan characteristic curves (head and efficiency curves) are examined experimentally. The comparison of the aerodynamic of two fans is completed with numerical simulation of flow patterns inside the volutes and around the rotors of fans.

The acoustical behavior of the fans is conducted experimentally. For this purpose, sound pressure level of the fans is investigated following the induct noise measurement approach. This scheme results in acoustical frequency spectrum of the fans. To improve the comparison of sound generation of the fans, pressure fluctuations on the volute of the fans are also studied experimentally. In this way, the main aerodynamic sound source of the fans (forces acting on casing) will be provided.

2. NUMERICAL PROCEDURE

To examine the difference between single and double outlet fans from the point of view of fluid flow, numerical tests are considered. The governing equations for turbulent flow in the fans are continuity and Reynolds-averaged Navier-Stokes equations as follows:

$$\frac{\partial u_i}{\partial x_i} = 0 \quad (1)$$

$$\rho \frac{\partial u_j u_i}{\partial x_j} = \frac{\partial}{\partial x_j} \left[-P \delta_{ij} + \mu \left(\frac{\partial u_i}{\partial x_j} + \frac{\partial u_j}{\partial x_i} \right) - \rho \overline{u'_i u'_j} \right] \quad (2)$$

Where u_i and u_j are mean velocity components while u'_i and u'_j are fluctuating velocities. The standard k-ε turbulence model is used to model Reynolds stress term ($\rho \overline{u'_i u'_j}$), following the previous work by the authors (Montazerin *et al.* 2015):

$$\frac{\partial}{\partial x_i} (\rho k u_i) = \frac{\partial}{\partial x_i} \left[\left(\mu + \frac{\mu_t}{\sigma_k} \right) \frac{\partial k}{\partial x_j} \right] + G_k - \rho \varepsilon + 1.44 \quad (3)$$

$$\frac{\partial}{\partial x_i} (\rho \varepsilon u_i) = \frac{\partial}{\partial x_i} \left[\left(\mu + \frac{\mu_t}{\sigma_\varepsilon} \right) \frac{\partial \varepsilon}{\partial x_j} \right] + 1.44 \frac{\varepsilon}{k} G_k - 1.92 \rho \frac{\varepsilon^2}{k} + 1.92 \quad (4)$$

$$\mu_t = 0.09 \rho \frac{k^2}{\varepsilon}, \quad G_k = \mu_t \left(\frac{\partial u_j}{\partial x_i} + \frac{\partial u_i}{\partial x_j} \right) \frac{\partial u_j}{\partial x_i} \quad (5)$$

All the geometry (as shown in Fig. 4) and boundary conditions are discussed in the previous work by the authors (Montazerin *et al.* 2015). To achieve grid-independent numerical results, single and double outlet fans at maximum flow rate operation are numerically simulated with different number of mesh elements. The results show that for 1,200,000 and 1,600,000 mesh elements for single and double outlet fans respectively, less than 0.1% change in fan efficiency is observed. The fan efficiency is subsequently defined in eq. (9), where rotor torque in numerical simulation is used instead of power of electronic motor in experimental procedure. The fan

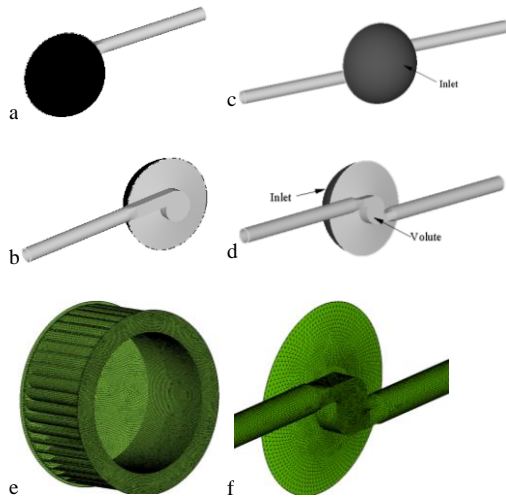


Fig. 4. Computational domain in numerical simulation of the fans; a: single outlet fan, front view b: single outlet fan, back view; c: double outlet fan, front view d: double outlet fan, back view e: mesh on the rotor f: mesh on the volute and outlets.

efficiency is an appropriate parameter for grid independence study, since is including three different parameters (pressure, flow rate, and forces acting on the rotor).

3. EXPERIMENTAL TEST SETUP

3.1 Centrifugal Fan Facility

A single inlet / double outlet fan, fan 1, and a single inlet / single outlet squirrel cage fan, fan 2, were constructed to investigate the performance and sound generation in centrifugal fans and compare the effect of two main sound sources (volute tongues) on the fan sound level. Figure 5 depicts schematically double and single outlet fans and their components.

Geometrical dimensions of the rotor, volute and inlet are selected based on the previous studies (Damangir and Montazerin 1998; Hessami Azizi *et al.* 2005; Montazerin *et al.* 2000; Nikkhoo *et al.* 2009). The dimensions of the fans are in Table 1. The same rotor and impeller – cutoff clearance is used in these fans. The volute profile is designed according to the following exponential equation which is a well-known formula for squirrel cage fans (Montazerin *et al.* 2015):

$$r = r_s \exp(\theta \times \tan(\alpha_s)) \tag{6}$$

where r_s , θ , α_s , and r , are radius of the start of the scroll, volute angle, volute spread angle, and volute radius, respectively.

Table 1 Key dimensions of the fans

Fan Type	Fan 1	Fan 2
(double outlet)	×	
(single outlet)		×
Rotor		
Rotor inner diameter: D_1	285 (mm)	285 (mm)
Rotor outer diameter: D_2	350 (mm)	350 (mm)
Rotor width: b	165 (mm)	165 (mm)
Number of blades: Z	43	43
Blade inlet angle: β_1	90°	90°
Blade outlet angle: β_2	155°	155°
Rotational speed: N	740 (rpm)	740 (rpm)
Volute		
Angle of start of volute: θ_s	30°	30°
Volute spread angle: α_s	5°	5°
Radius of start of the cutoff: r_s	200 (mm)	200 (mm)
Volute width: B	200 (mm)	200 (mm)
Height of the outlet: h	140 (mm)	250 (mm)
Radius of the volute tongue tip: r_v	15 (mm)	15 (mm)
Cutoff clearance: $d_s (=D_2/2 - r_s)$	25 (mm)	25 (mm)
Inlet		
Radius of inlet tip: $r_{in\ tip}$	15 (mm)	15 (mm)
Inlet diameter: D_{inlet}	295 (mm)	295 (mm)

3.2 Performance Test Apparatus

The experimental test facility was built following free inlet / ducted outlet arrangement proposed in ISO 5801 (1997) for performance measurements and plotting the characteristics curves of the fans. This choice is because of application of squirrel cage fans as air supplier at entrance of HVAC (heating, ventilating and air-conditioning) channels. Figure 6 shows a schematic of the test setup. As shown in figure two, outlet channels of double outlet fan are named upper and lower channels. These channels are connected to circular PVC ducts by canvas connections, while regulation cones are used outside and in front of each duct to control the exit flow rate. Experiments on the flow rate and efficiency of fans are carried out using a Pitot tube, placed into both upper and lower test ducts following the instructions presented in ISO 5801, and therefore in double outlet cases, the flow rate of each outlet is individually measured. The results show approximately similar flow rate in both channels for the same throttle setting. A similar test setup with one channel is used for single outlet fan.

The ambient conditions and also uncertainties in the measurements are:

- Ambient pressure: 88650 Pa
- Dry-bulb temperature: 22 °C

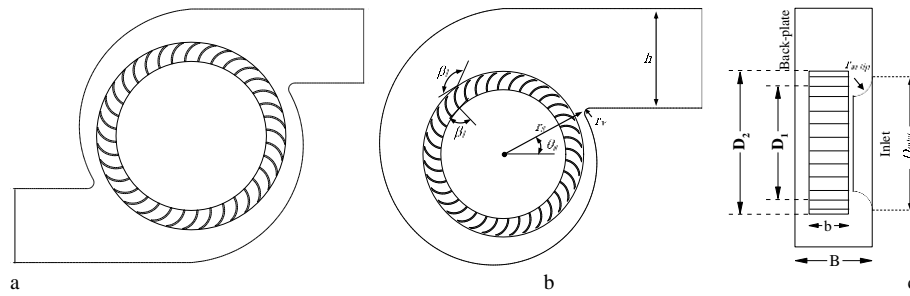


Fig. 5. A schematic of front view of (a) double outlet, (b) single outlet squirrel cage fans, and (c) side view of a single outlet type with the dimensions.

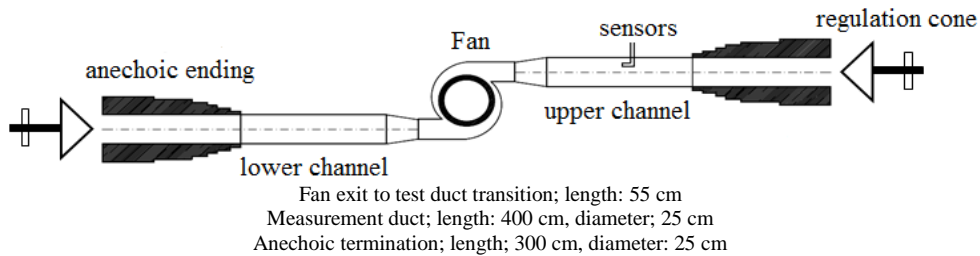


Fig. 6. A schematic of the test installation (sensors are microphone, Pitot tube, and thermometer).

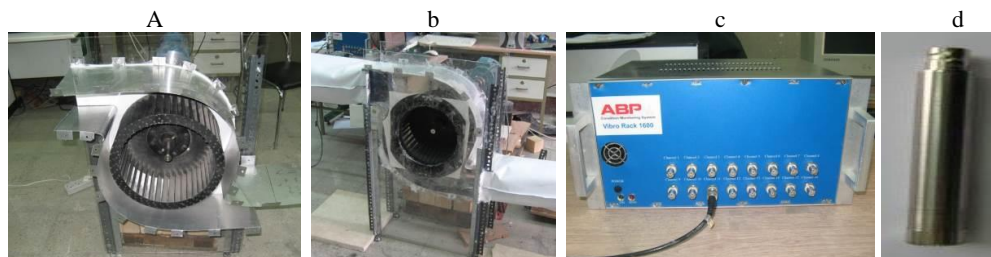


Fig. 7. Test set and measurement devices, (a) double outlet fan after installation, (b) double outlet fan connected to the ducts, (c) data acquisition front, (d) microphone.

- Wet-bulb temperature: 15 °C
- Pitot tube (pressure): $\pm 1.5\%$
- Thermometer: $\pm 1^\circ\text{C}$
- Barometer (ambient pressure): $\pm 0.5\%$
- Total pressure coefficient: 1.23%
- Efficiency: 1.65%

3.3 Noise Measurement Setup and Tools

Investigation of the sound generation of the fans is carried out in a standardized ducted installation with free inlet / ducted outlet arrangement according to [ISO 5136 \(2003\)](#). This setup is similar to that for performance measurements (Fig. 6). Anechoic terminations shown in Fig. 6 removed undesired noise reflections at the end of both channels. These terminations are constructed of rock wool with stepped expansion.

The acoustic pressure generated by the fan is measured by a 1/2" diameter microphone produced by BSWA Technology Company, model MPA 261 with uncertainty of ± 0.2 dB. This microphone is protected by a foam ball that faced the air-stream

like a windshield and reduced wind-generated noise. The microphone data is collected by a dedicated computer. In [ISO 5136 \(2003\)](#) minimum data acquisition time for frequencies lower than 160 Hz and higher than 200 Hz is proposed to be 30 and 10 second, respectively.

A view of the test setup, data collection setup and microphone are shown in Fig. 7. Also the microphone is flush-mounted on holes presented in Fig. 8 on the mid plane of volute in order to measure the surface pressure fluctuations as the main sound source (similar to [Velarde-Suárez et al. 2006](#)).

4. FAN PERFORMANCE AND CHARACTERISTICS CURVE

It is common to employ the rotor inlet area ($\pi D^2/4$) and rotor tip velocity (πDn) in calculation of dimensionless parameters for comparison of different squirrel cage fans ([Montazerin et al. 2015](#)). The flow and head coefficients for squirrel cage fans, based on the above mentioned parameters, are then defined as:

$$\begin{aligned} \phi &= \frac{Q}{\text{Velocity Scale} \times \text{Surface Scale}} \\ &= \frac{Q}{(\pi n D) (\pi D^2 / 4)} = \frac{4Q}{\pi^2 D^3 n} \end{aligned} \quad (7)$$

$$\begin{aligned} \psi &= \frac{\Delta P_t}{\frac{1}{2} \rho (\text{Velocity Scale})^2} = \frac{\Delta P_t}{\frac{1}{2} \rho (\pi n D)^2} \\ &= \frac{2 \Delta P_t}{\rho \pi^2 n^2 D^2} \end{aligned} \quad (8)$$

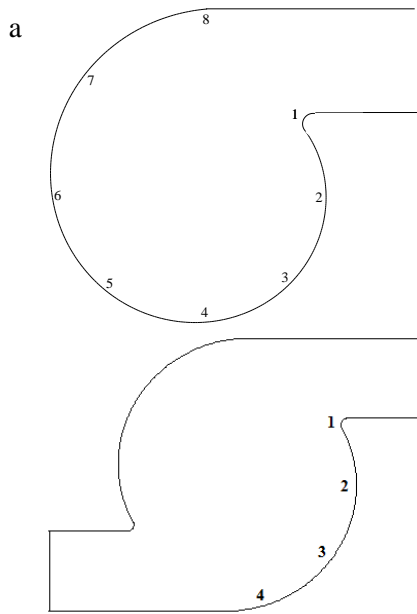


Fig. 8. Point of measurement of pressure fluctuations on the mid plane of the (a) single outlet and (b) double outlet squirrel cage fan

where n , Q and ΔP_t are rotational speed (in rps), fan volumetric flow rate and total pressure respectively. Also fan efficiency is defined by:

$$\eta = \frac{k_p \Delta P_t Q}{PR} \quad (9)$$

where k_p is a compressibility coefficient defined in ISO 5801 (1997) and PR is power of the electric motor. There is no standard method to combine pressure rise and flow rates of the two outlet channels of double outlet squirrel cage fans for calculation of the efficiency and head coefficients. In the present work, the total efficiency of double outlet fan is calculated for the total flow rate that exits both upper and lower outlets while the total pressure is calculated for each outlet channel individually. Therefore Q and ΔP_t in Eqs. (7-9) are individual to each outlet channel, and the fan efficiency is calculated from the following:

$$\eta = \frac{(k_p \Delta P_t Q)_{\text{lower ch.}} + (k_p \Delta P_t Q)_{\text{upper ch.}}}{PR} \quad (10)$$

Figure 9 shows variation of efficiency, η , and total

pressure coefficient, ψ , versus flow coefficient, ϕ , of the fans considered in this article. The double outlet fan results correspond to the outlets with similar settings. As it was mentioned before, the efficiency of double outlet fans is obtained for the total flow rate that exit from both upper and lower outlets.

Figure 9-a demonstrates the efficiency curves where the single and double outlet fans have similar behavior with flow rate. The best efficiency point (BEP) of fan 1 corresponds to the flow coefficient $\phi = 0.6$ (approximately $\phi = 0.3$ for each outlet channel) with $\eta = 0.5$; while that for fan 1 occurs at $\phi = 0.4$. The maximum and minimum flow of fan 1 is twice those of fan 2. It means that the flow of each channel of double outlet fan is equal to the single outlet one for similar throttle settings. From another view point it can be concluded that for the same rotor size, the flow rate obtained by a double outlet volute is twice a single outlet one, while the efficiency has no considerable change.

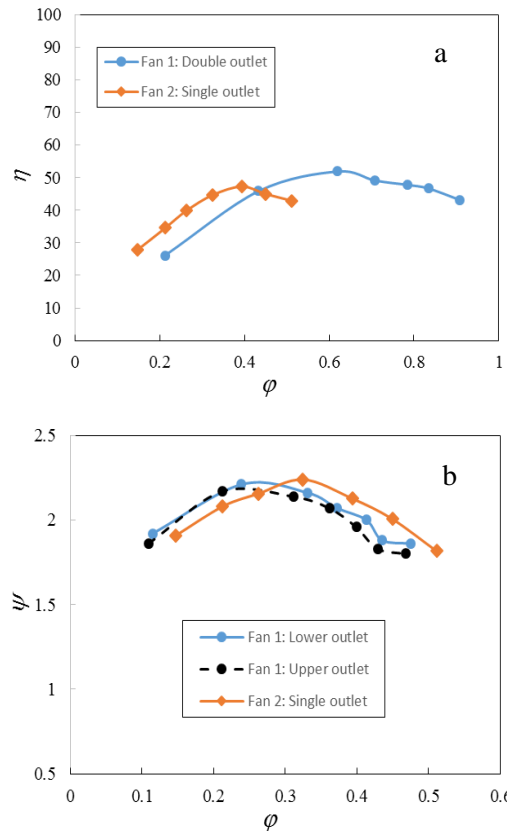


Fig. 9. Variations of (a) efficiency and (b) total pressure coefficient, versus traditional flow coefficient.

The curves in Fig. 9-b agree with general behavior of single outlet forward curved blade centrifugal fans (Cory 2005; Damangir 2004; Velarde-Suárez et al. 2013). The zone with positive slope (for flow rates lower than BEP) are susceptible to unstable aerodynamic phenomena that could be responsible for increase in noise generation and decrease in

performance. Some of these phenomena are the flow rotation behind the fan inlet and flow separation in the blade channels (Neise 1992). General behavior of the curve of the double outlet fan is similar to that of single outlet one. At flow rates lower than BEP the double outlet fan produces higher pressures than the single outlet one; while at higher ϕ a different trend is found.

The characteristics curves of the used squirrel cage fans show that when two consumers use a single air-conditioning system, a double outlet squirrel cage fan that supplies flow rate twice a single outlet type can be used. In other words, the consumers in Fig. 3-a receives only half the fresh air of those in Fig. 3-b, for the same rotor with similar geometrical parameters and rotational speed.

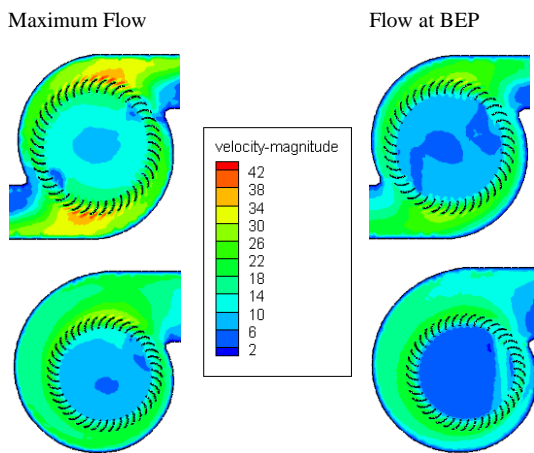


Fig. 10. Fluid flow (velocity magnitude) in middle plane of fans at maximum flow rate (left) and flow at BEP (right).

To clarify the observations in the two previous figures, velocity magnitude in middle plate of the fans at maximum flow rate and BEP is presented in Fig. 10. Exit flow from the rotor is observed in the regions near the fan outlet channel for two fans. In the double outlet fan, two active regions (regions with jet/wake flow) are found (each region is near each outlet) and therefore each outlet behaves similar to a single outlet fan, and subsequently, total flow of double outlet fan is twice that of single outlet one. At BEP, rotor active region of single outlet fan is wider than the double outlet fan and therefore higher flow coefficient and efficiency is observed for single outlet fans at BEP.

5. SOUND GENERATION ANALYSIS

5.1 Data Collection and Evaluation of Power Spectrum

Two components are important in the study of sound generation of fans: sound pressure level at blade passing frequency (BPF) that is named tonal noise, and total sound pressure level (total SPL or total noise) that is sound level of root square of all components in the sound pressure frequency

spectrum. The BPF of the present rotor is approximately 530 Hz. In this study the data acquiring time and frequency are 33 second and 8000 Hz, subsequently any acoustic phenomena with maximum frequency of 4000 Hz are detectable in the experiments.

After executing the FFT algorithm on sound pressure data, the sound pressure level can be calculated (in dB) from the following equation:

$$SPL = 10 \log \left(\frac{P^2}{P_{ref}^2} \right) \quad (11)$$

where P is sound pressure component in the power spectrum and P_{ref} is reference pressure that is equal to 20 μ Pa. Total noise is obtained by sum level of sound pressures in the spectrum according to:

$$SPL_{\Sigma} = 10 \log \left(\frac{P_1^2 + P_2^2 + \dots + P_m^2}{P_{ref}^2} \right) \quad (12)$$

Noise measurements are carried out in sensor position (Fig. 6) at radius equal to half of the duct radius and three different peripheral positions with 120° angular distance from each other. The average sound pressure level (SPL_{ave}) is calculated from the following, after the noise measurements (ISO 5136, 2003):

$$SPL_{ave} = 10 \log \left(\frac{1}{m} \sum_{i=1}^m 10^{0.1SPL_i} \right) \quad (13)$$

where SPL_i is the sound pressure level in i^{th} position and m is number of measurement positions.

5.2 Sound Generation Behavior

Figure 11 illustrates frequency spectra of sound pressure level of fans at four different volumetric flow rates from lowest to highest. The trend of spectra is similar to those of similar fans in the literature (Velarde-Suárez *et al.* 2009). High intensity noise at low frequency (especially at rotor frequency RF and around it) is evident for all cases in these figures. This broadband low frequency noise is expected in this type of ducted test setup, as stated by Velarde-Suárez *et al.* (2009), and is not annoying for human ear.

There is also a peak at the blade passing frequency (BPF = 530 Hz) for two fans, that its amplitude varies with flow rate. This noise component is called aerodynamic tonal noise or BPF noise. The main source of BPF noise is interaction of the jet/wake rotor flow with the volute. Since the intensity of the jet and wake flow and also the length of the volute dealing with this flow varies with flow rate, the BPF noise varies with the volumetric flow rate too. First harmonic of the BPF noise is observed in two fans at low flow rates ($Q = 0.15$ and 0.31 for fan 1 & $Q = 0.19$ and 0.28 for fan 2). This noise component disappears between broadband noises at high volumetric flow rates especially for fan 1. The only peak noise at high flow rates in fan 1 is BPF component.

Another observation in these figures is decreasing

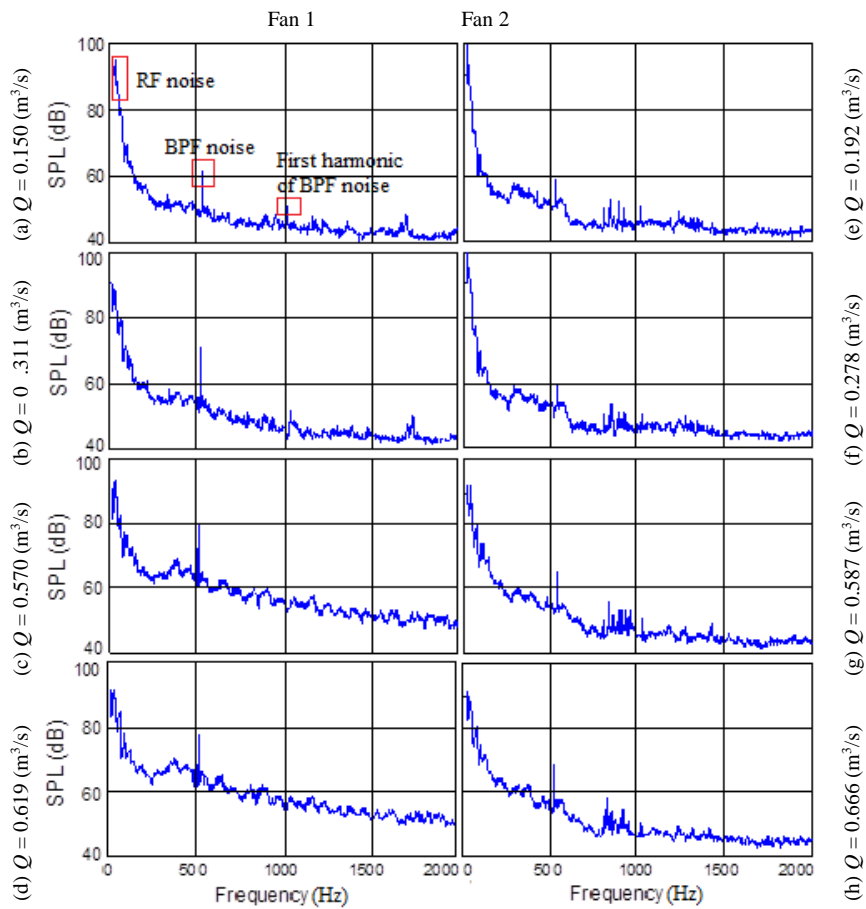


Fig. 11. Frequency spectra of SPL at the outlet channel of fan 1 (lower outlet) and 2.

SPL power spectrum by increasing the frequency. This behavior, that is commonplace in power density spectrum of noise in the centrifugal fans, shows minor effects of high frequency phenomenon in sound generation.

A stronger broadband SPL is observed for two fans at minimum flow rate. *Fehse and Neise (1999)* showed that this noise is due to flow separation in the blade suction side. At minimum flow rate both outlet channels are almost closed and the circulating flow occurs in the inlet region of the fan. Such noise disappears with increase of volumetric flow rate and distinct amplitudes are evident only at BPF.

In the power spectrum of fan 2, noticeable SPL is observed at frequencies between 800 to 1000 Hz, which is not the case for double outlet fan. *Velarde-Suárez et al. (2008)* suggested that this could correspond to fan resonance to the vibration of fan components, especially the volute, and are not related to any aerodynamic phenomena. Since double and single outlet fans have different casings, such noise is not observed in fan 1.

Variation of the total and tonal noise in two fans versus flow rate is depicted in Fig. 12 to achieve better comparison. According to Fig.12-a, for double outlet fan (fan1) maximum SPL occurs at

minimum flow rate, then a decrease in SPL is observed by increasing flow rate. When this fan operates close to the BEP, minimum or moderate SPL is generated. The single outlet fan reveals a different sound generation behavior. In this fan, minimum SPL occurs at lowest and highest flow rates, while highest SPL corresponds to moderate flow rates. This observation is thoroughly different from fan 1 with minimum SPL at BEP. The flow rate that exits from each of the outlets of double outlet fans, is equal to that for a single outlet fan, and the lower total SPL of these fans compared to a single outlet type are preferable for application of these fans in engineering systems.

According to Fig. 12-b, the BPF noise of double outlet fan is higher than that of single outlet one in the entire operating range. Also the results show that the BPF noise of fans is an increasing function of flow rate. According to the literature (*Montazerin et al. 2015*), higher SPL at BPF corresponds to larger jet and wake profile along the rotor exit near the volute tongue.

As it was observed previously the flow rate in each channel of the double outlet fan is equal to the flow rate of single outlet fan. Therefore, the flow velocity in outlet channels of fan 1 is higher than that of fan 2, because of the smaller outlet width of

fan 1 compared to fan 2. The stronger fluid flow and subsequently higher pressure fluctuation generated on the cut-off of double outlet fans, results in higher SPL at blade passing frequency.

Also the velocity magnitude in middle plane of the fans (Fig. 10) shows that in the region near the outlet of fan 1, the volute – rotor distance is smaller than that in fan 2 while the velocity magnitude is higher. Consequently, in double outlet fans the tonal noise can be generated in other parts of the volute in addition the cut-off. To clarify this phenomena, relative static pressure in middle plane of the fans is presented in Fig. 13. It can be seen in the figure that in fan 2 an approximately uniform flow pattern is found around the parts of volute far from the cut-off, while in fan1 it is not the case.

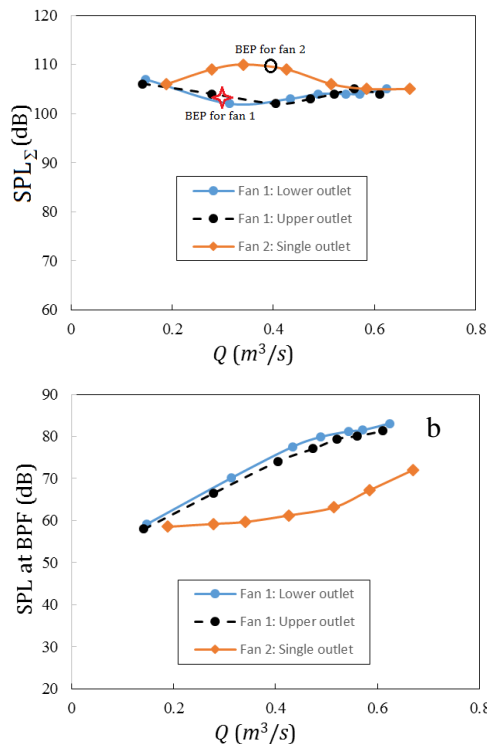


Fig. 12. Comparison of (a) SPL_{Σ} and (b) blade passing frequency noise of fan 1 and 2.

To further clarify the observation of two last figures, the amplitude of pressure fluctuations on the mid plane of the fans (according to the points shown in Fig. 8) at blade passing frequency is shown in Fig.14. The results of the single outlet fan show decreasing pressure amplitude from the volute tongue to point 7, while an increasing pressure occurs from point 7 to point 8, above the rotor where exit flow from the rotor faces to the volute. The order of pressure amplitude at point 8 is equal to that at the volute tongue region. Therefore, it can be concluded that the main source of tonal noise in the single outlet fan is close to volute tongue.

From the comparison of the results of fan 1 and 2, the highest pressure amplitude of the double outlet fan occurs at point 2 (about 20° far from the cutoff). Moreover the order of the pressure amplitude in fan

2 is approximately 4 times fan 1. The higher flow velocity of rotor flow and smaller rotor-volute gap in double outlet fan compared to the single outlet one are responsible for this phenomena. Consequently the higher pressure amplitude is responsible for the higher BPF noise of fan 2 in comparison with the single outlet fan.

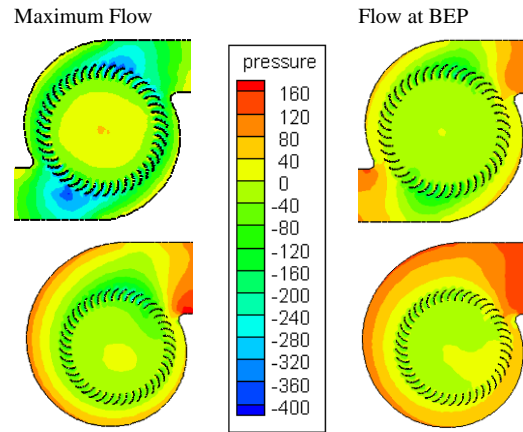


Fig. 13. Relative static pressure in middle plane of fans at maximum flow rate (left) and flow of BEP (right).

6. CONCLUSION

In the present work a numerical study on fluid flow and an experimental study on the performance and sound generation in single inlet / double outlet and also single inlet / single outlet squirrel cage fans was carried out. The experiments show that the total flow rate of double outlet fan is approximately twice that for single outlet, while a similar efficiency is observed. In another words, each outlet channel of the double outlet fan operates similar to a single outlet fan.

The acoustic results show that tonal noise in both fans is an increasing function of exit flow rate, while double outlet fan has a higher BPF noise approximately at all operating range. The numerical results show higher velocity magnitude at the exit of the rotor in double outlet fan that results in larger zones of volute affected by jet and wake flow in double outlet fan in comparison with the single outlet one. The higher tonal noise in double outlet fan compared to the single outlet one is due to: (1) stronger jet and wake flow and consequently higher pressure fluctuations around the cut-off, and (2) larger zone of volute affected by pressure fluctuations compared to the single outlet fan.

Also it is found that the tonal noise sources in single outlet fan are (1) the cutoff region, and (b) the volute portion above the rotor.

Finally from a practical point of view it can be concluded that in cases that noise problem is not important, using double outlet squirrel cage fan instead of a single outlet one, twice flow rate is provided.

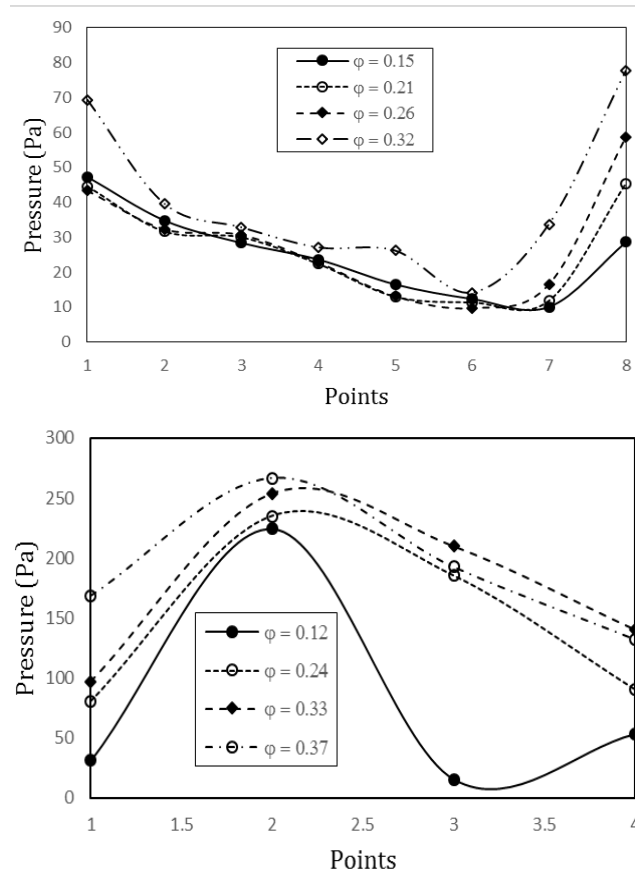


Fig. 14. Pressure fluctuation amplitude at blade passing frequency on the mid plane of the volute of (a) single outlet and (b) double outlet squirrel cage fan.

ACKNOWLEDGEMENTS

The authors would like to thank Dr. Abdolreza Ohadi Hamadani for providing the sound measuring laboratory equipment.

REFERENCES

- Bleier, F. P. (1998). *Fan Handbook, Selection, Application, and Design*. USA: McGraw-Hill.
- Cory, W. T. W. (2005). *Fans & Ventilation; A Practical Guide*. Elsevier.
- Damangir, A. (2004). *Joint impeller/scroll sizing of squirrel cage fans using alternative non-dimensional head and flow rate coefficients (In Persian)*, PhD thesis, Amirkabir University of Technology, Tehran, Iran.
- Damangir, A. and N. Montazerin (1998). Stall cells inside the volute of a squirrel-cage fan. *in Integrated Design and Process Technology*, IDPT, 5, USA.
- Fehse, K. R. and W. Neise (1999). Generation mechanisms of low-frequency centrifugal fan noise. *AIAA Journal* 37, 1173–1179.
- Gao, M., P. Dong, Sh. Lei and A. Turan (2017). Computational Study of the Noise Radiation in a Centrifugal Pump When Flow Rate Changes. *Energies* 10(2), 1-11.
- Gu, Y., D. Qi, Y. Mao and X., Wang (2011). Theoretical and experimental studies on the noise control of centrifugal fans combining absorbing liner and inclined tongue. *Proceedings of the Institution of Mechanical Engineers, Part A: Journal of Power and Energy* 225 789-801.
- Hessami Azizi, M. H., N. Montazerin and A. Damangir (2005). A combined noise-laser doppler velocimetry study of the squirrel-cage fan. *Iranian Journal of Mechanical Engineering* 6, 5-17.
- Jiang, B., H. Liu, B. Li and J. Wang (2018) Effects of cut volute profile on squirrel cage fan performance and flow field. *Advances in Mechanical Engineering* 10(3), 1-14.
- Jian, Ch., H. Yuan, G. Li, W. Canxing, Ch. Liu and L. Yuanrui (2018). Aerodynamic noise prediction of a centrifugal fan considering the volute effect using IBEM. *Applied Acoustics* 132, 182–190.
- Joonga, K. S., S. H. Jina, S. Wallinc and A. V.

- Johanssonc (2019). Design of the centrifugal fan of a belt-driven starter generator with reduced flow noise. *International Journal of Heat and Fluid Flow* 76, 72–84.
- Liu, Ch., Y. Cao, W. Zhang, P. Ming and Y. Liu (2019). Numerical and experimental investigations of centrifugal compressor BPF noise. *Applied Acoustics* 10, 290–301.
- Liu, H., H. Dai, J. Ding, M. Tan, Y. Wang and H. Huang (2016). Numerical and experimental studies of hydraulic noise induced by surface dipole sources in a centrifugal pump. *Journal of Hydrodynamics* 28(1), 43-51.
- Montazerin, N., A. Damangir and A. Kazemifard (2001). A study of slip factor and velocity components at the rotor exit of forward-curved squirrel cage fans, using laser Doppler anemometry. *Proceedings of the Institution of Mechanical Engineers, Part A: Journal of Power and Energy* 215, 453-463.
- Montazerin, N., A. Damangir and H. Mirzaei (2000). Inlet induced flow in squirrel-cage fans. *Proceedings of the Institution of Mechanical Engineers, Part A: Journal of Power and Energy* 214, 243-253.
- Montazerin, N., G. Akbari and M. Mahmoodi (2015). *Developments in Turbomachinery Flow, Forward Curved Centrifugal Fans*, Woodhead Publishing, Elsevier.
- Neise, W. (1992). Review of fan noise generation mechanisms and control methods. in *Proceedings of the SFA Symposium on Fan Noise*, 1992: Senlis, France.
- Nikkhoo, M., N. Montazerin, A. Damangir and R. S. Samian (2009). An experimental study of leaning blades on the half-cone rotor of a squirrel cage fan. *Proceedings of the Institution of Mechanical Engineers, Part A: Journal of Power and Energy* 223(8), 973-980.
- Paramasivam, K., S. Rajoo, A. Romagnoli and W.J. Yahya (2017). Tonal noise prediction in a small high speed centrifugal fan and experimental validation. *Applied Acoustics* 125, 59–70.
- Qi, D., M. Yijun, L. Xiaoliang and Y. Minjian (2009). Experimental study on the noise reduction of an industrial forward-curved blades centrifugal fan. *Applied Acoustics* 70, 1041–1050.
- Qi, G.W. and Zh. Wei (2017). Noise reduction mechanisms for the inclined leading edge vaned diffuser in a centrifugal fan. *Proceedings of the Institution of Mechanical Engineers, Part A: Journal of Power and Energy* 231(1), 68–83.
- The International Organization for Standardization, ISO 5136 (2003). *Acoustics-Determination of sound power radiated into a duct by fans and other air-moving devices-in-duct method*.
- The International Organization for Standardization, ISO 5801 (1997). *Industrial fans, Fan performance testing using standardized airways*.
- Velarde-Suárez S., R. Ballesteros-Tajadura, J. González-Pérez and B. Pereiras-García (2009). Relationship between volute pressure fluctuation pattern and tonal noise generation in a squirrel-cage fan. *Applied Acoustics* 70, 1384–1392.
- Velarde-Suárez, S., C. Santolaria-Morros and R. Ballesteros-Tajadura (1999). Experimental study on the aeroacoustic behavior of a forward-curved blades centrifugal fan. *ASME Journal Fluids Engineering* 121, 271-281.
- Velarde-Suárez, S., F. Guerras-Colón, R. Ballesteros-Tajadura, J. González, K. M. Argüelles Díaz, J. M. Fernández Oro and C. Santolaria-Morros (2013). Evaluation of design criteria for squirrel-cage fans used in public transport HVAC systems. *HVAC&R Research* 19, 363–375.
- Velarde-Suárez, S., R. Ballesteros-Tajadura, C. Santolaria-Morros and B. Pereiras-Garcia (2008). Reduction of aerodynamic tonal noise of a forward-curved centrifugal fan by modification of volute tongue geometry. *Applied Acoustics* 69, 225-232.
- Velarde-Suárez, S., R. Ballesteros-Tajadura, J. P. Hurtado-Cruz and C. Santolaria-Morros (2006). Experimental determination of the tonal noise sources in a centrifugal fan. *Journal of Sound and Vibration* 295, 781-796.
- Wang, K., Y. Ju and C. Zhang (2018). Numerical investigation on flow mechanisms of squirrel cage fan. *Proceedings of the Institution of Mechanical Engineers, Part A: Journal of Power and Energy*.
- Xu, C. and Y. Mao (2016a). Experimental investigation of metal foam for controlling centrifugal fan noise. *Applied Acoustics* 104, 182–192.
- Xu, C. and Y. Mao (2016b). Passive control of centrifugal fan noise by employing open-cell metal foam. *Applied Acoustics* 103, 10–19.
- Zhang, Q., Y. Mao, H. Zhou, C. Zhao, Q. Diao and D. Qi (2018). Vibro-acoustics of a pipeline centrifugal compressor Part II. Control with the micro-perforated panel. *Applied Acoustics* 132, 152-166.
- Zhoua, H., Y. Mao, Q. Zhang, C. Zhao, D. Qi and Q. Diao (2018). Vibro-acoustics of a pipeline centrifugal compressor part I. Experimental study. *Applied Acoustics* 131, 112–128.